European Journal of Pharmaceutical Sciences 63 (2014) 45–52

Contents lists available at ScienceDirect

European Journal of Pharmaceutical Sciences

journal homepage: www.elsevier.com/locate/ejps

A physiologically based pharmacokinetic model for Valproic acid in adults and children

Kayode Ogungbenro *, Leon Aarons, the CRESim & Epi-CRESim Project Groups

Centre for Applied Pharmacokinetic Research, Manchester Pharmacy School, The University of Manchester, Oxford Road, Manchester M13 9PT, United Kingdom

ARTICLE INFO

Article history:
Received 24 March 2014
Received in revised form 22 May 2014
Accepted 29 June 2014
Available online 7 July 2014

Keywords:
Valproic acid
Pharmacokinetics
Dravet syndrome
Epilepsy
PBPK
Modelling

ABSTRACT

Valproic acid is an anti-convulscant drug that is widely used in the treatment of different types of epilepsy and since its introduction the clinical use has increased rapidly both as a sole agent and in combination therapies. The mechanism of action has been linked to blockade of voltage-dependent sodium channels and potentiation of GABAergic transmission. The most widely used route of administration of Valproic acid is oral, although it can also be given intravenously and rectally and its pharmacokinetics has been studied extensively. The aim of this work was to develop a physiologically based pharmacokinetic model for plasma and tissue/organ prediction in children and adults following intravenous and oral dosing of Valproic acid. The plasma/tissue concentration profile will be used for clinical trial simulation in Dravet syndrome, a rare form of epilepsy in children where the combination of Valproic acid, stiripentol and clobazam has shown remarkable results. A physiologically based pharmacokinetic model was developed with compartments for gut lumen, enterocyte, gut tissue, systemic blood, kidney, liver, brain, spleen, muscle and rest of body. System and drug specific parameters for the model were obtained from the literature from *in vitro* and *in vivo* experiments. The model was initially developed for adults and scaled to children using age-dependent changes in anatomical and physiological parameters and ontogeny functions for enzyme maturation assuming the same elimination pathways in adults and children. The results from the model validation showed satisfactory prediction of plasma concentration both in terms of mean prediction and variability in children and adults following intravenous and oral dosing especially after single doses. The model also adequately predicts clearance in children. Due to limited distribution of Valproic acid into tissues, the concentration in plasma is about 8–9 times higher than tissues/organs. The model could help to improve clinical outcome in the treatment of Dravet syndrome through dose optimisation.

1. Introduction

Valproic acid (VPA) is an anti-convulscant drug that is widely used in the treatment of different types of epilepsy including simple and generalised epilepsies (Levy et al., 1990). Since it was introduced over 50 years ago, its clinical use has increased rapidly both as a sole agent and in combination with other anti-epileptic drugs. The mechanism of action of VPA is still unknown although it has been linked to blockade of voltage-dependent sodium channels and potentiation of GABAergic transmission (Suzuki et al., 2011). The most widely used route of administration of VPA is oral, although it can also be given intravenously and rectally. Oral formulations include syrup, oral solutions, plain tablets, capsules, enteric-coated tablets and slow release formulations (Zaccara et al., 1988).

The pharmacokinetics (PK) of VPA has been investigated using different formulations. The absorption of VPA is rapid from the gastrointestinal tract, the maximum concentration in plasma is reached within 4 h of administration of a tablet formulation (Zaccara et al., 1988). Absorption after oral administration from the gastrointestinal tract is also complete as with other extravascular administrations (Bialer et al., 1985; Zaccara et al., 1988). VPA distributes mainly into the extracellular space with minor tissue uptake and low apparent volume of distribution (Klotz and Antonin, 1977). The volume of distribution at steady state (V_{ss}) is around 10*L* (8.4 ± 3.4*L* (Klotz and Antonin, 1977), 12.6 ± 1.2*L* (Nitsche and Mascher, 1982) and 8.2*L* (6.9 – 10*L*) (Bryson et al., 1983)). The metabolism of VPA is complex and it is mainly by glucuronidation and oxidation, and more than 15 metabolites of VPA have been detected in urine, these accounted for 85% ± 19.5% of the

* Corresponding author. Tel.: +44 161 275 2355; fax: +44 161 275 8349.
E-mail address: kayode.ogungbenro@manchester.ac.uk (K. Ogungbenro).

http://dx.doi.org/10.1016/j.ejps.2014.06.023
0928-0987/

administered dose with almost no excretion of the unchanged drug (Levy et al., 1990). Glucuronidation is the most important route for the elimination of VPA, it accounts for 30–70% of the administered dose (Argikar and Remmel, 2009). VPA is glucuronidated by UGTs to form acyl glucuronides that are excreted in urine. Mitochondria β-oxidation is another important route for the elimination of VPA, it accounts for 20–40% of the administered dose (Argikar and Remmel, 2009). CYP450 enzymes (CYP2A6, 2B6 and 2C9) are responsible for elimination of about 10% of the administered dose (Argikar and Remmel, 2009; Levy et al., 1990). The half-life of VPA is around 12 h in adults (Klotz, 1977; Klotz and Antonin, 1977; Nitsche and Mascher, 1982; Perucca et al., 1978a; Perucca et al., 1978b). VPA is highly bound (over 90%) mostly to albumin in plasma: two binding sites have been identified on the albumin molecule for VPA binding (Zaccara et al., 1988). The binding of VPA in plasma is saturable with the free fraction of the drug higher at high total plasma concentration and there have been a number of attempts in the literature to characterise the non-linear binding kinetics of VPA (Cloyd et al., 2003; Scheyer et al., 1990; Suzuki et al., 2011; Ueshima et al., 2009, 2011). Although VPA is considered to be generally safe, it has been associated with rare but fatal hepatotoxicity which is associated with a number of risk factors (Ho et al., 2003). Although the mechanism of the toxicity remains unknown it has been associated with one of the metabolites: 4-ene-VPA which is produced via CYP450 enzymes (Ho et al., 2003; Levy et al., 1990; Sadeque et al., 1997). Therapeutic drug monitoring is therefore often used in the clinical use of VPA to monitor plasma concentration, especially free plasma concentration, to prevent toxicities.

In a clinical study, a remarkable result was achieved by a combination of VPA, stiripentol (STI) and clobazam (CLB) in the treatment of Dravet Syndrome (DS) (Chiron et al., 2000). DS also known as severe myoclonic epilepsy in infants is a rare form of epilepsy that affects at least 1 in 40,000 children up to the age of 7 years and accounts for about 7% of severe forms of epilepsy in children under the age of 3 years (Hurst, 1990; Morse, 2011). DS is associated with serious deleterious effects on cognitive and motor development and the seizures associated with DS are known to be some of the most resistant to conventional therapies. The effectiveness of the combination of VPA, STI and CLB represents an important breakthrough in the treatment of DS.

The aims of this work were to develop a physiologically based pharmacokinetic model (PBPK) for VPA to predict plasma and tissue concentration in adults and children and to investigate changes in plasma and tissue concentrations with age. This work forms part of the CRESim (Child Rare Euro-Simulation) project designed to investigate the use of modelling and simulation in the development of drugs for the treatment of rare diseases. In this case the focus is on DS and the drugs under investigation are CLB, STI and VPA. The PBPK model developed for the prediction of plasma and tissue concentrations of VPA in the present study will be used in combination with the PBPK model developed for STI and CLB and combined with DS disease model developed under other work packages to obtain a PBPK-PD model for clinical trial simulation.

2. Methodology

The approach used in the development of a PBPK model for adults and children is to develop and validate the model first in adults and then scale to children using age-dependent changes in anatomical and physiological functions such as organ/tissue flows and volumes and enzyme maturation functions. This is similar to a workflow published recently to support the paediatric research and development using a PBPK model and Lorazepam as a case study (Maharaj et al., 2013).

2.1. PBPK model development and assumptions

The PBPK model developed for VPA is made up of 10 compartments: gut lumen, enterocyte, gut tissue, systemic blood, kidney, liver, brain, spleen, muscle and rest of body. The rest of body compartment is used to account for mass balance of the system. Tissues/organs of the PBPK model were modelled using flow limited assumption described using Eq. (1)

$$V_T \frac{dC_T}{dt} = Q_T \left(C_b - \frac{C_T}{K_{p,T}} \right) \quad (1)$$

where V_T, C_T, Q_T and $K_{p,T}$ are the volume, concentration, blood flow, tissue/blood concentration ratio for the different tissues and C_b is the systemic blood concentration. For intravenous dosing, the drug is added directly to the systemic blood compartment and for oral dosing the drug is added to the gut lumen compartment from where it is absorbed by a first order process via the gut wall and the liver into the systemic circulation. It was assumed that VPA is metabolised by glucuronidation, β-oxidation and CYP450 enzymes. Glucuronidation of VPA is assumed to be by UGT2B7 and it occurs in the gut, kidney and liver (Argikar and Remmel, 2009; Soars et al., 2002). β-oxidation and CYP450 metabolism take place in the liver. It was assumed that VPA is metabolised by β-oxidation into 2(E)-ene-valproic acid (2(E)-ene-VPA) and by CYP2C9 into three metabolites: 4-ene-valproic acid (4-ene-VPA), 4-hydroxyl valproic acid (4-OH VPA) and 5-hydroxyl valproic acid (5-OH VPA) (Levy et al., 1990; Sadeque et al., 1997). The saturable non-linear binding of VPA to plasma albumin was accounted for by a two site binding model taken from the literature (Cloyd et al., 2003).

2.2. System parameters

Systems parameters for adults (assumed to be 18–20 years old and 70 kg weight) were obtained from the literature (Valentin, 2002). These include organ/tissue weights and volumes, cardiac output (CO), body surface area (BSA), height (HT), body weight (BW) and haematocrit (HCT). Table 1 shows organ/tissue volumes and blood flows for adults.

2.2.1. Drug specific parameter

Tissue/blood concentration ratios (K_p) for the tissues were predicted using the equations proposed by Rodgers and Rowland and

Table 1
Organ/tissue volumes (V), blood flows (Q) and tissue/blood concentration ratio (K_p) obtained using Rodgers and Rowland equation for different tissues/organs in adults.

Parameters	Organs/tissues								
	Systemic blood	Kidney	Liver	Gut	Enterocyte	Brain	Spleen	Muscle	Rest of body
V (L)	5.3	0.31	1.8	1.7	0.12	1.45	0.15	29	–[a]
Q (L/h)	356.31[b]	79.5	25.38	54.6	21.38	46.8	11.7	66.3	–[c]
K_p	–	0.32	0.23	0.36	–	0.17	0.25	0.52	0.40

[a] $70 - \Sigma V_T$.
[b] Cardiac output.
[c] $CO - \Sigma Q_T$.

Table 2
Drugs specific parameter values used for describing the kinetics of Valproic acid.

Parameter	Description	Value	References
MW (g)	Molecular weight	144.21	–
B/P	Blood/plasma concentration ratio	0.55	Soars et al. (2002), Loscher (1978)
fa	Fraction absorbed from the gut	1	Klotz and Antonin (1977)
ka (h^{-1})	Absorption rate constant	2.0	Dutta et al., (2007)
V_{ss} (L)	Volume of distribution at steady state	~10	Klotz and Antonin (1977), Nitsche and Mascher (1982), Bryson et al. (1983)
CL (L/h)	*In vivo* clearance	~0.53	Soars et al. (2002), Levy et al. (1990)
$Clint_{gluc\_int}$ (L/h)	Intestinal intrinsic clearance (glucuronidation)	0.0091	Soars et al. (2002)
$Clint_{gluc\_ren}$ (L/h)	Renal intrinsic clearance (glucuronidation)	7.09	Soars et al. (2002), Levy et al. (1990)
$Clint_{gluc\_hep}$ (L/h)	Hepatic intrinsic clearance (glucuronidation)	1.25	Soars et al. (2002), Levy et al. (1990)
$Clint_{\beta\text{-}oxid}$ (L/h)	Hepatic intrinsic clearance (β-oxidation)	7.61	Levy et al. (1990)
$Clint_{4ene\_VPA}$ (L/h)	Hepatic intrinsic clearance (4-ene-VPA)	0.043	Levy et al. (1990)
$Clint_{4OH\_VPA}$ (L/h)	Hepatic intrinsic clearance (4OH-VPA)	1.10	Levy et al. (1990)
$Clint_{5OH\_VPA}$ (L/h)	Hepatic intrinsic clearance (5OH-VPA)	0.82	Levy et al. (1990)
N1	Number of binding sites per class (Site 1)	1.54	Cloyd et al. (2003)
K1 (mM)	Binding affinity constant (Site 1)	11.9	Cloyd et al. (2003)
N2	Number of binding sites per class (Site 2)	0.194	Cloyd et al. (2003)
K2 (mM)	Binding affinity constant (Site 2)	164	Cloyd et al. (2003)

are presented in Table 1 (Rodgers et al., 2005; Rodgers and Rowland, 2006). K_p for the rest of body was obtained by lumping other tissues that have not been accounted for explicitly in the model. The predicted K_ps were also adjusted using an empirical scalar so that the predicted and observed V_{ss} matches. Intrinsic clearance parameters: intestinal glucuronidation ($Clint_{gluc\_int}$), renal glucuronidation ($Clint_{gluc\_ren}$), hepatic glucuronidation ($Clint_{gluc\_hep}$) and hepatic β-oxidation ($Clint_{\beta\text{-}oxid}$) and hepatic intrinsic clearance parameters for the metabolism of VPA into 4-ene-VPA ($Clint_{4ene\_VPA}$), 4-OH VPA ($Clint_{4OH\_VPA}$) and 5-OH VPA ($Clint_{5OH\_VPA}$) metabolites by CYP2C9 were obtained from the literature (Table 2). Parameters (*N*1 and *N*2, the number of binding sites per class of binding site and *K*1 and *K*2, the binding affinity constants) that describe the non-linear kinetics of VPA binding to plasma albumin using two binding sites were also obtained from the literature (Table 2). Other drug specific parameters used in the PBPK model obtained from the literature are listed in Table 2.

2.2.2. Paediatric scaling

System parameters for children were obtained from the literature to scale the model from adults to children. Reference values for different paediatric age groups (0, 1, 5, 10 and 15 years) were obtained from the literature to account for anatomical and physiological changes in parameters such as organ/tissue volumes and blood flows (Valentin, 2002). Age-dependent changes in body size descriptors such as BW and HT were also obtained from the literature and these were used to predict BSA using the Haycock and Dubois equation (DuBois and DuBois, 1916; Haycock et al., 1978). CO in children was predicted using the equation proposed by Johnson et al. (2006). Simple linear interpolation was used to scale organ/tissue volumes and blood flows for ages in between the reference values.

The binding kinetics were assumed to be the same in children as in adults, but plasma albumin levels were adjusted in children based on the equations proposed by Johnson et al. (2006). The same K_ps were used in adults and children for all the tissues. Metabolic pathways were scaled to children by using the ontogeny function for the enzyme responsible or allometry. $Clint_{gluc\_int}$, $Clint_{gluc\_ren}$ and $Clint_{gluc\_hep}$ were scaled by using the ontogeny function for UGT2B7 (Edginton et al., 2006), $Clint_{4ene\_VPA}$, $Clint_{4OH\_VPA}$ and $Clint_{5OH\_VPA}$ were scaled by using the ontogeny function for CYP2C9 (Salem et al., 2013) and $Clint_{\beta\text{-}oxid}$ was scaled by using allometry (West et al., 1999).

2.2.3. Variability

Variability was introduced on both system and drug specific parameters in the PBPK model. Variability on system parameters was introduced in the model mostly via BW and HT. Cardiac output in the model was defined as a function of BSA and through this variability was introduced into plasma/organ blood flows in the PBPK model. Variability on organ/tissue volumes was introduced via BW. Variability was also introduced on drug specific parameters such as *ka*, $Clint_{gluc\_int}$, $Clint_{gluc\_ren}$, $Clint_{gluc\_hep}$, $Clint_{4ene\_VPA}$, $Clint_{4OH\_VPA}$, $Clint_{5OH\_VPA}$, $Clint_{\beta\text{-}oxid}$, *N*1, *N*2, *K*1 and *K*2. A lognormal distribution was assumed for all parameter with a coefficient of variation of 20%.

2.2.4. Simulation

For the assessment of the performance of the developed PBPK model, simulated plasma concentrations were compared with

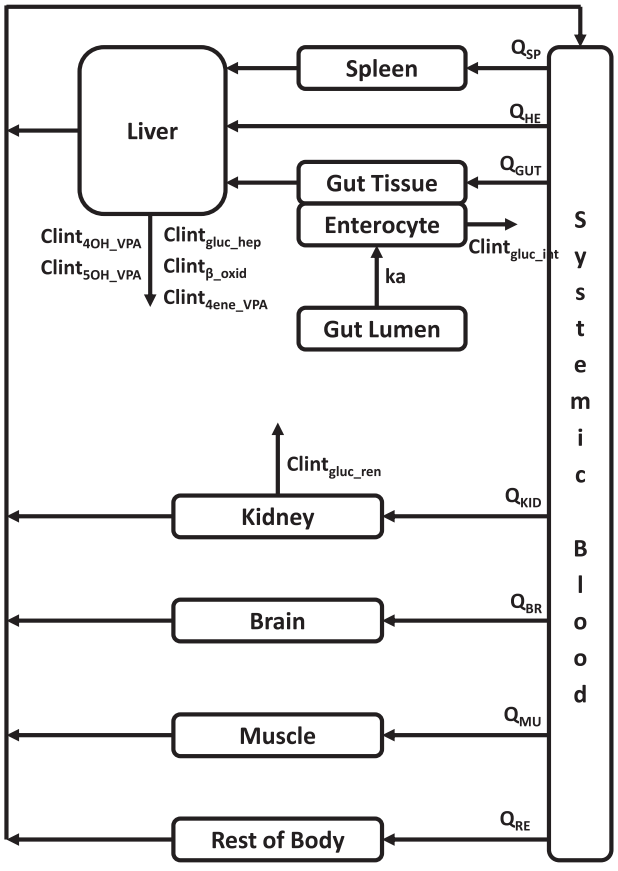

Fig. 1. Schematic representation of the PBPK model for VPA.

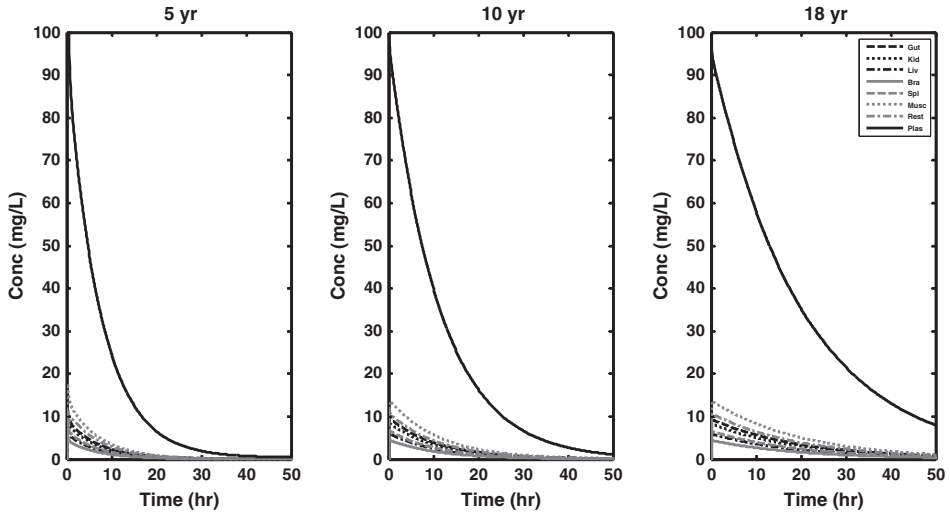

Fig. 2. Simulated median concentration–time profiles of Valproic acid in gut (Gut), kidney (Kid), liver (Liv), brain (Bra), spleen (Spl), muscle (Musc), rest of body (Rest) and plasma (Plas) following intravenous dosing of 15 mg/kg in 5, 10 and 18 years old subjects.

observed plasma concentration data from different published studies. Simulations were based on the reported distribution of age, BW and dose in the corresponding studies. A virtual simulation of 1000 subjects was simulated in all cases and the 95% prediction interval (2.5th, 50th and 97.5th percentiles) were plotted and superimposed with the published plasma concentration data. Individual plasma concentration data reported in tables were copied or individual data reported as profiles or mean data with standard deviation or standard error reported as bars were digitized using GetData Graph Digitizer (2013). The simulations were made to match published studies in terms of dose and other study design factors.

3. Results

The developed PBPK model is shown in Fig. 1 and the differential equations that implement this model are shown in the Appendix A. Figs. 2 and 3 show simulated median concentration–time profiles of VPA in plasma and different tissues (gut, kidney, liver, brain, spleen, muscle, rest of body) of the PBPK model in 5, 10 and 18 years old subjects following intravenous and oral dosing of 15 mg/kg dose. The figures show that the concentration of VPA in plasma is about 8–9 times higher than the concentration in tissues/organs in adults and children. The plasma and tissue/organ profiles in the subjects also show an exponential decline with the fastest decline observed in the 5 years old subject followed by the 10 years old subject.

Observed plasma concentration data and simulated plasma concentration–time profiles (median and 95% prediction intervals) after bolus intravenous doses in adults are shown in Fig. 4. The data were obtained from two published studies. The data in Fig. 4a was obtained from six healthy adult volunteers who received 800 mg of VPA (Perucca et al., 1978a) and the data in Fig. 4b was obtained from six healthy adult volunteers who received 1000 mg of VPA (Nitsche and Mascher, 1982). Observed plasma concentration data from two studies and simulated plasma concentration–time profiles (median and 95% prediction intervals) after single oral doses in adults are shown in Fig. 5. The data in Fig. 5a was obtained from six healthy adult volunteers who received 800 mg of VPA (Perucca et al., 1978a) and the data in Fig. 5b was obtained from six healthy adult volunteers who

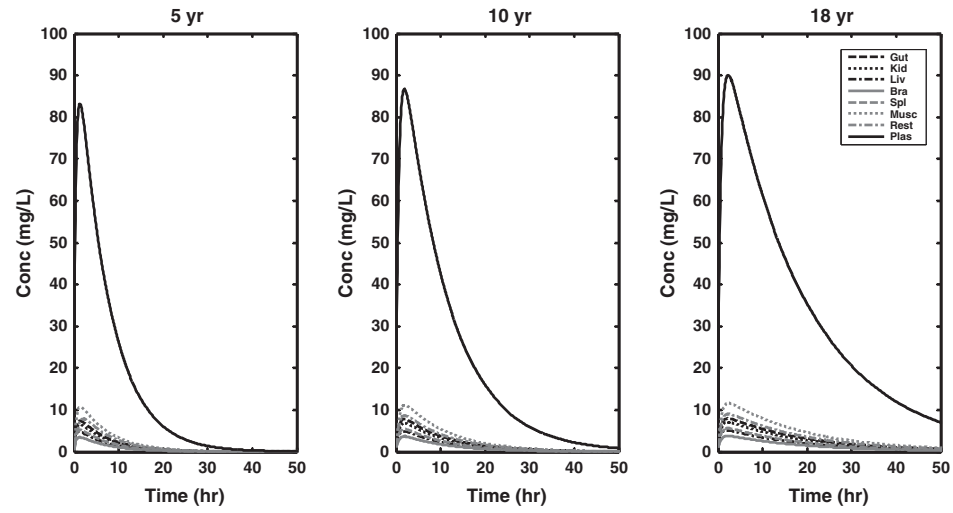

Fig. 3. Simulated median concentration–time profiles of Valproic acid in gut (Gut), kidney (Kid), liver (Liv), brain (Bra), spleen (Spl), muscle (Musc), rest of body (Rest) and plasma (Plas) following oral dosing of 15 mg/kg in 5, 10 and 18 years old subjects.

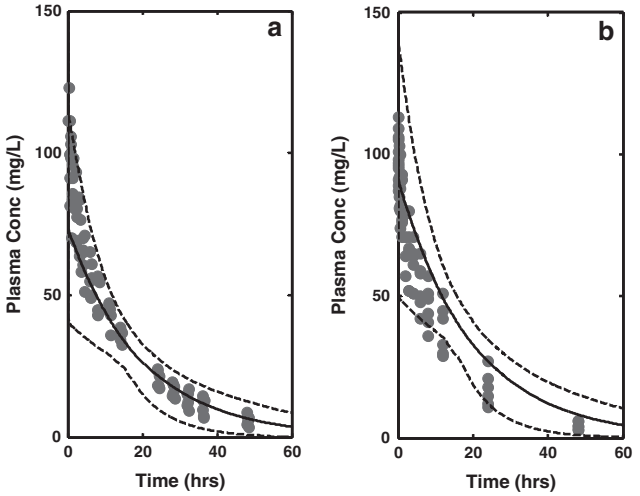

Fig. 4. Observed plasma data and simulated plasma concentration–time profiles (2.5th, 50th and 97.5th percentiles) of Valproic acid after intravenous dose in adults (a) 800 mg (Perucca et al., 1978a), (b) 1000 mg (Nitsche and Mascher, 1982).

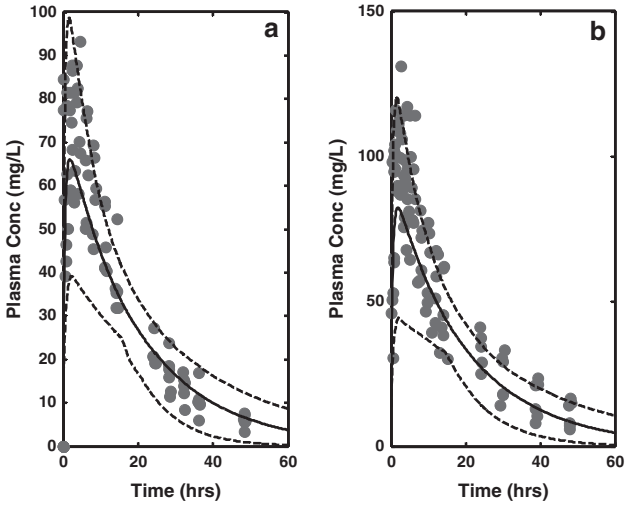

Fig. 5. Observed plasma data and simulated plasma concentration–time profiles (2.5th, 50th and 97.5th percentiles) of Valproic acid after oral dose in adults (a) 800 mg (Perucca et al., 1978a), (b) 1000 mg (Bialer et al., 1985).

received 1000 mg of VPA (Bialer et al., 1985). Fig. 6 shows observed plasma concentration data and simulated plasma concentration–time profiles (2.5th, 50th and 97.5th percentiles) of VPA after multiple oral doses in twelve healthy adult volunteers who received 900 mg twice daily (Fig. 6a) and six healthy adult volunteers who received 1000 mg twice daily (Fig. 6b) (Nitsche and Mascher, 1982).

Data on plasma clearance of VPA in children were obtained from the literature and compared with simulated 95% prediction interval as a function of age. Metabolic pathways were scaled to children by using the ontogeny functions for the enzymes responsible and allometry as described under scaling above. Plasma clearance values were obtained from four different clinical studies in children with epilepsy who were receiving VPA as a monotherapy. Data from patients with co-medication of VPA and any other antiepileptic drug were excluded from the analysis. Fig. 7a shows data from Chiba et al. (1985) in twenty-one children, Cloyd et al. (1993) also in twenty-one children and Hall et al. (1985) in thirteen children. Fig. 7b shows data from Bondareva et al. (2004) in 141 subjects.

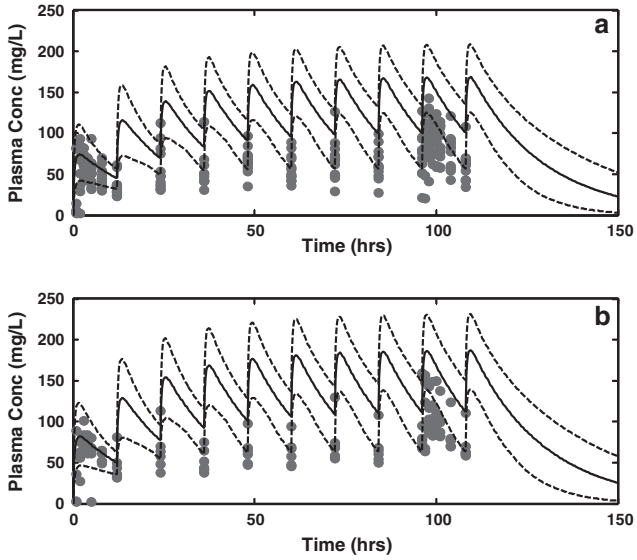

Fig. 6. Observed plasma data and simulated plasma concentration–time profiles (2.5th, 50th and 97.5th percentiles) of Valproic acid after multiple oral doses in adults (Nitsche and Mascher, 1982), (a) 900 mg twice daily (b) 1000 mg twice daily.

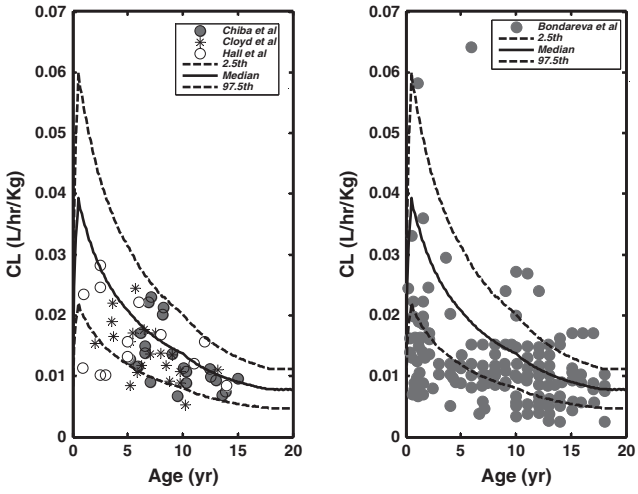

Fig. 7. Observed clearance from different studies and predicted clearance-age profiles (2.5th, 50th and 97.5th percentiles) of Valproic acid in children (a) Chiba et al. (1985), Cloyd et al. (1993) and Hall et al. (1985), (b) Bondareva et al. (2004).

Observed plasma concentration data and simulated plasma concentration–time profiles (median and 95% prediction intervals) after a bolus intravenous dose in children and adults with epilepsy who are on VPA monotherapy are shown in Fig. 8. The data in Fig. 8a was obtained from 10 children (1–17 year) who received 12–15 mg/kg VPA intravenously (Williams et al., 2012). The data in Fig. 8b was obtained from 11 Thai epileptic children (1–15 year) who received 15–20.5 mg/kg VPA intravenously (Visudtibhan et al., 2011) and the data in Fig. 8c was obtained from 112 adults and children with epilepsy (1–79 year) who received 15 mg/kg VPA intravenously (Cloyd et al., 2003). Fig. 9 shows observed data and simulated plasma concentration–time profiles (2.5th, 50th and 97.5th percentiles) of VPA in epileptic children who received 20–60 mg/kg/day VPA orally for at least 3 weeks (Lundberg et al., 1982). Fig. 9a shows data for 7 children (one subject on 4 occasions) who received VPA twice daily and Fig. 9b shows data for 4 children who received VPA thrice daily.

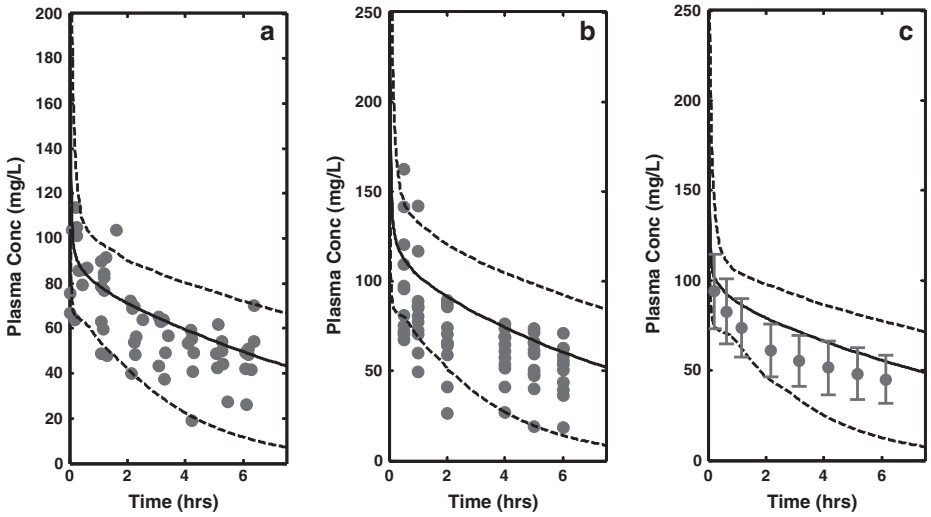

Fig. 8. Observed plasma data and simulated plasma concentration–time profiles (2.5th, 50th and 97.5th percentiles) of Valproic acid in children after a single intravenous dose in children (a) Williams et al., 2012, (b) Visudtibhan et al. (2011), (c) Cloyd et al. (2003).

4. Discussion

This work has described a PBPK model for the prediction of plasma and tissue/organ concentrations following intravenous and oral dosing in adults and children for the purpose of clinical trial simulation. The model was first developed and validated in adults and then scaled to children using age-dependent changes in anatomical, physiological and drug specific parameters. The same approach has been used and advocated for the purpose of drug development in children because more information is available in adults compared to children (Barrett et al., 2012; Edginton, 2011; Jiang et al., 2013; Leong et al., 2012). The PBPK model developed has compartments for key organs/tissues and accounted for different specific issues that have been investigated and reported to be important for the PK of VPA in humans. Non-linear binding of VPA to plasma albumin has been reported in a number of studies and parameters describing this relationship were obtained from the literature and implemented within the model. Also, parameters associated with different routes of elimination of VPA were obtained from the literature and implemented in the model. Some clearance parameters were reported as *in vivo* systemic clearance estimates in the publications, and these were converted into intrinsic clearances using the well stirred model (Rowland et al., 2010).

K_ps are very important component of a PBPK model, as they help to explain the tissue/organ distribution of drugs. Because they require tissue concentration data, experimentally determined values especially in humans are almost impossible to get. Values from preclinical species such as mice, rat, dog, and monkey are used whenever available. However when values from preclinical species are not available, equations have been developed for the prediction of K_ps using input parameters such as physicochemical properties of the drug, fraction unbound in plasma and blood/plasma ratio. In this work the equation proposed by Rodgers and Rowland have been used (Rodgers et al., 2005; Rodgers and Rowland, 2006) and the K_p for rest of body was obtained by lumping predicted K_ps for tissues that have not been explicitly accounted for in the model. The predicted K_ps were further scaled using an empirical scalar so that the predicted and observed V_{ss} matches. The predicted V_{ss} using the K_ps in Table 1 was 18.5L compared with observed values of 8.4 ± 3.4L (Klotz and Antonin, 1977), 12.6 ± 1.2L (Nitsche and Mascher, 1982) and 8.2(6.9 – 10L) (Bryson et al., 1983). Because the predicted V_{ss} is higher than the observed values, the K_ps were all scaled by a factor of 0.5 and the predicted V_{ss} is now 10.7L. It is not uncommon to scale predicted K_ps in PBPK modelling for the predicted and observed V_{ss} to match and there is an option in the PBPK model software Simcyp and others to do this (Jamei et al., 2009).

The predicted and observed V_{ss} show that VPA distributes mainly into the extracellular space with minor tissue uptakes which has also been observed *in vivo* (Klotz and Antonin, 1977) and this is also demonstrated in the high concentrations predicted in plasma compared to tissues/organs. The predicted profiles following intravenous and oral dosing in Figs. 2 and 3 respectively show that plasma concentrations are about 8–9 times higher than concentrations in tissues/organs, this is consistent with the limited distribution into tissues/organs. Higher concentrations in plasma relative to tissues/organs has also been observed experimentally in rabbits following intravenous dosing (Ichimura et al., 1985).

Intrinsic clearances for the different routes of elimination of VPA obtained from the literature for adults were scaled to children using ontogeny functions developed for the enzymes (CYP2C9 and UGT2B7) and allometry (β-oxidation) assuming the routes of elimination are the same in adults and children. The scaled intrinsic

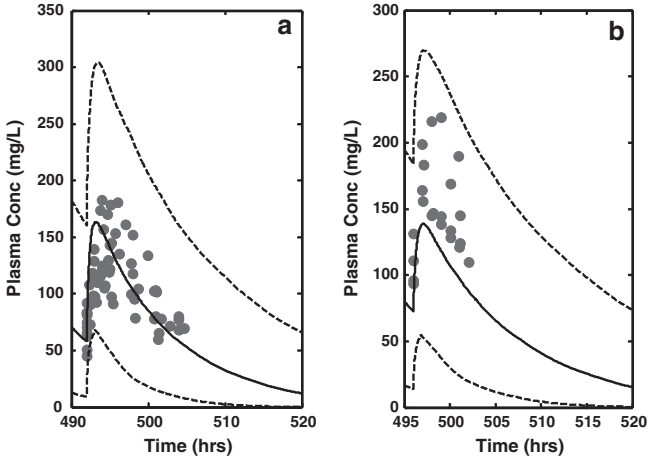

Fig. 9. Observed plasma data and simulated plasma concentration–time profiles (2.5th, 50th and 97.5th percentiles) of Valproic acid in children after multiple oral dose in children (Lundberg et al., 1982) (a) twice daily, (b) thrice daily.

clearances were converted to plasma whole body clearance using the well stirred model. The predicted VPA clearance against age in Fig. 7 shows how clearance is changing with age in children. The predicted 95% interval shows adequate coverage of the data obtained from three published studies in Fig. 7a, however it appears there is slight over-prediction of the data obtained from a single study in Fig. 7b especially for children less than 5 years old. This is possibly related to the activity of UGT2B7 which is responsible for more than 50% of the metabolism of VPA and it was assumed the adult value is reached around 1 year of age. The profiles in Fig. 7 shows that the median clearance of VPA expressed in L/h/kg is slightly higher at birth than adult values and increases rapidly until it reaches a maximum around 6 months of age and then starts to decrease exponentially until adulthood.

The predicted plasma concentration intervals in adults and children following intravenous and oral dosing showed satisfactory coverage of the data obtained from published studies in the literature. The plots for adults after oral and intravenous single doses in Figs. 4 and 5 are satisfactory however the prediction following multiple oral doses in Fig. 6 show slight over prediction of the data by the PBPK model. One possible explanation for this is the auto-induction of the β-oxidation pathway which leads to reduced plasma concentrations following chronic dosing of VPA. This has been demonstrated in healthy volunteers where following chronic dosing plasma concentrations as well as urinary recovery of VPA and its metabolites were monitored (McLaughlin et al., 2000). This phenomenon has not been included in the present model and therefore represents an area for future expansion. This will require further investigation and characterisation of the mechanism and parameters of the auto-induction process using an *in vitro* system. The prediction for children obtained following single intravenous doses (Fig. 8) and multiple oral doses (Fig. 9) also show satisfactory coverage of the observed clinical data in all cases. This shows that the age-related changes in system and drugs specific parameters as well as scaling for the different metabolic routes and assumptions are reasonable. The prediction intervals in Fig. 9 are wider because of the wide range of doses used in the original studies which were matched in the simulations. Although oral predictions of the model have focused on plain tablets, the model can be used to predict other oral formulations of VPA that are available by making necessary changes to the absorption rate constant, as it has been shown that the differences in absorption characteristics of the different formulations of VPA can be adequately accounted for by using different rate constants (Dutta and Reed, 2007; Williams et al., 2012).

The approach that has been used in this work to predict and scale distribution and elimination is mechanistic, using the knowledge of anatomy and physiology to explain the PK of VPA. Empirical methods such as allometry (West et al., 1997) have also been proposed, Edginton (2011) provided merits, flaws and limits of allometry and mechanism based approaches.

5. Conclusion

In conclusion, a PBPK model that describes the PK of VPA has been developed for plasma and tissue concentration prediction in adults and children following intravenous and oral dosing. Validation of the model using published plasma concentration data showed satisfactory prediction in adults and children. The model could help to improve clinical outcome in the treatment of DS and other epileptic conditions through dose optimisation.

Acknowledgements

This work was performed as part of Child-Rare-Euro-Simulation project. CRESim was funded by the ERA-NET PRIOMEDCHILD Joint Call in 2010. Members of the CRESim Project Group: Leon Aarons; Agathe Bajard; Clément Ballot; Yves Bertrand; Frank Bretz; Daan Caudri; Charlotte Castellan; Sylvie Chabaud; Catherine Cornu; Frank Dufour; Nathalie Eymard; Roland Fisch; Renzo Guerrini; Vincent Jullien; Behrouz Kassaï; Patrice Nony; Kayode Ogungbenro; David Pérol; Gérard Pons; Harm Tiddens; Anna Rosati. Members of the Epi-CRESim Project Group: Corinne Alberti; Catherine Chiron; Catherine Cornu, Polina Kurbatova; Rima Nabbout.

The authors also acknowledge helpful discussions with Dr Aleksandra Galetin, Dr Michael Gertz, Dr Eleanor Howgate, Dr Henry Pertinez, Mr Nikolaos Tsamandouras, Mr Adam Darwich and member of Centre for Applied Pharmacokinetic Research, Manchester Pharmacy School.

Appendix A

(1) Gut

Lumen

$$\frac{dA_{LUM}}{dt} = -kaA_{LUM}$$

Enterocyte

$$V_{ENT}\frac{dC_{ENT}}{dt} = kaA_{LUM} - Q_{ENT}C_{ENT} - Clint_{gluc\_int}C_{ENT}$$

Tissue

$$V_{GUT}\frac{dC_{GUT}}{dt} = (Q_{GUT} + Q_{ENT})\left(C_P - \frac{C_{GUT}}{K_{p,GUT}}\right)$$

(2) Systemic Blood

$$V_P\frac{dC_P}{dt} = \frac{(Q_{HE} + Q_{GUT} + Q_{ENT} + Q_{SP})C_{LIV}}{K_{p,LIV}} + \frac{Q_{KID}C_{KID}}{K_{p,KID}} + \frac{Q_{MU}C_{MU}}{K_{p,MU}} + \frac{Q_{BR}C_{BR}}{K_{p,BR}} + \frac{Q_{RE}C_{RE}}{K_{p,RE}} + Q_{HE} + Q_{GUT} + Q_{ENT} + Q_{KID} + Q_{MU} + Q_{BR} + Q_{SP} + Q_{RE})C_P$$

(3) Kidney

$$V_{KID}\frac{dC_{KID}}{dt} = Q_{KID}\left(C_P - \frac{C_{KID}}{K_{p,KID}}\right) - \frac{Clint_{gluc\_ren}C_{KID}fub}{K_{p,KID}}$$

(4) Liver

$$V_{LIV}\frac{dC_{LIV}}{dt} = Q_{HE}\left(C_P - \frac{C_{LIV}}{K_{p,LIV}}\right) + \frac{(Q_{GUT} + Q_{ENT})C_{GUT}}{K_{p,GUT}} - \frac{(Q_{GUT} + Q_{ENT})C_{LIV}}{K_{p,LIV}} + \frac{Q_{SP}C_{SP}}{K_{p,SP}} - \frac{Q_{SP}C_{LIV}}{K_{p,LIV}} + Q_{ENT}C_{ENT} - \frac{(Clint_{gluc,hep} + Clint_{\beta,oxid} + Clint_{2ene,VPA} + Clint_{4OH,VPA} + Clint_{5OH,VPA})C_{LIV}fub}{K_{p,LIV}}$$

(5) Brain

$$V_{BR}\frac{dC_{BR}}{dt} = Q_{BR}\left(C_P - \frac{C_{BR}}{K_{p,BR}}\right)$$

(6) Spleen

$$V_{SP}\frac{dC_{SP}}{dt} = Q_{SP}\left(C_P - \frac{C_{SP}}{K_{p,SP}}\right)$$

(7) Muscle

$$V_{MU}\frac{dC_{MU}}{dt} = Q_{MU}\left(C_P - \frac{C_{MU}}{K_{p,MU}}\right)$$

(8) Rest of body

$$V_{RE}\frac{dC_{RE}}{dt} = Q_{RE}\left(C_P - \frac{C_{RE}}{K_{p,RE}}\right)$$

References

Argikar, U.A., Remmel, R.P., 2009. Effect of aging on glucuronidation of valproic acid in human liver microsomes and the role of UDP-glucuronosyltransferase UGT1A4, UGT1A8, and UGT1A10. Drug Metab. Dispos. 37 (1), 229–236.

Barrett, J.S., Della Casa Alberighi, O., Laer, S., Meibohm, B., 2012. Physiologically based pharmacokinetic (PBPK) modeling in children. Clin. Pharmacol. Ther. 92 (1), 40–49.

Bialer, M., Hussein, Z., Raz, I., Abramsky, O., Herishanu, Y., Pachys, F., 1985. Pharmacokinetics of valproic acid in volunteers after a single dose study. Biopharm. Drug Dispos. 6 (1), 33–42.

Bondareva, I.B., Jelliffe, R.W., Sokolov, A.V., Tischenkova, I.F., 2004. Nonparametric population modeling of valproate pharmacokinetics in epileptic patients using routine serum monitoring data: implications for dosage. J. Clin. Pharm. Ther. 29 (2), 105–120.

Bryson, S.M., Verma, N., Scott, P.J., Rubin, P.C., 1983. Pharmacokinetics of valproic acid in young and elderly subjects. Br. J. Clin. Pharmacol. 16 (1), 104–105.

Chiba, K., Suganuma, T., Ishizaki, T., Iriki, T., Shirai, Y., Naitoh, H., Hori, M., 1985. Comparison of steady-state pharmacokinetics of valproic acid in children between monotherapy and multiple antiepileptic drug treatment. J. Pediatr. 106 (4), 653–658.

Chiron, C., Marchand, M.C., Tran, A., Rey, E., d'Athis, P., Vincent, J., Dulac, O., Pons, G., 2000. Stiripentol in severe myoclonic epilepsy in infancy: a randomised placebo-controlled syndrome-dedicated trial. STICLO study group. Lancet 356 (9242), 1638–1642.

Cloyd, J.C., Dutta, S., Cao, G., Walch, J.K., Collins, S.D., Granneman, G.R., Depacon Study, G., 2003. Valproate unbound fraction and distribution volume following rapid infusions in patients with epilepsy. Epilepsy Res. 53 (1–2), 19–27.

Cloyd, J.C., Fischer, J.H., Kriel, R.L., Kraus, D.M., 1993. Valproic acid pharmacokinetics in children. IV. Effects of age and antiepileptic drugs on protein binding and intrinsic clearance. Clin. Pharm. Ther. 53 (1), 22–29.

DuBois, D., DuBois, E.F., 1916. A formula to estimate the approximate surface area if height and weight be known. Arch. Int. Med. 17 (6_2), 863–871.

Dutta, S., Reed, R.C., 2007. Distinct absorption characteristics of oral formulations of valproic acid/divalproex available in the United States. Epilepsy Res. 73 (3), 275–283.

Edginton, A.N., 2011. Knowledge-driven approaches for the guidance of first-in-children dosing. Pediatr. Anesthesia 21 (3), 206–213.

Edginton, A.N., Schmitt, W., Voith, B., Willmann, S., 2006. A mechanistic approach for the scaling of clearance in children. Clin. Pharmacokinet. 45 (7), 683–704.

Hall, K., Otten, N., Johnston, B., Irvine-Meek, J., Leroux, M., Seshia, S., 1985. A multivariable analysis of factors governing the steady-state pharmacokinetics of valproic acid in 52 young epileptics. J. Clin. Pharmacol. 25 (4), 261–268.

Haycock, G.B., Schwartz, G.J., Wisotsky, D.H., 1978. Geometric method for measuring body surface area: a height–weight formula validated in infants, children, and adults. J. Pediatr. 93 (1), 62–66.

Ho, P.C., Abbott, F.S., Zanger, U.M., Chang, T.K.H., 2003. Influence of CYP2C9 genotypes on the formation of a hepatotoxic metabolite of valproic acid in human liver microsomes. Pharmacogenomics J. 3 (6), 335–342.

Hurst, D.L., 1990. Epidemiology of severe myoclonic epilepsy of infancy. Epilepsia 31 (4), 397–400.

Ichimura, F., Deguchi, Y., Yokogawa, K., Yamana, T., 1985. Physiologically based pharmacokinetics of valproic acid in rabbits. Int. J. Pharm. 27 (1), 45–60.

Jamei, M., Turner, D., Yang, J., Neuhoff, S., Polak, S., Rostami-Hodjegan, A., Tucker, G., 2009. Population-based mechanistic prediction of oral drug absorption. AAPS J. 11 (2), 225–237.

Jiang, X.L., Zhao, P., Barrett, J.S., Lesko, L.J., Schmidt, S., 2013. Application of physiologically based pharmacokinetic modeling to predict acetaminophen metabolism and pharmacokinetics in children. CPT: Pharmacomet. Syst. Pharmacol. 2, e80.

Johnson, T.N., Rostami-Hodjegan, A., Tucker, G.T., 2006. Prediction of the clearance of eleven drugs and associated variability in neonates, infants and children. Clin. Pharmacokinet. 45 (9), 931–956.

Klotz, U., 1977. Pharmacokinetic studies with Valproic acid in man. Arzneimittel-Forsch 27 (5), 1085–1088.

Klotz, U., Antonin, K.H., 1977. Pharmacokinetics and bioavailability of sodium valproate. Clin. Pharmacol. Ther. 21 (6), 736–743.

Leong, R., Vieira, M.L.T., Zhao, P., Mulugeta, Y., Lee, C.S., Huang, S.M., Burckart, G.J., 2012. Regulatory experience with physiologically based pharmacokinetic modeling for pediatric drug trials. Clin. Pharmacol. Ther. 91 (5), 926–931.

Levy, R.H., Rettenmeier, A.W., Anderson, G.D., Wilensky, A.J., Friel, P.N., Baillie, T.A., Acheampong, A., Tor, J., Guyot, M., Loiseau, P., 1990. Effects of polytherapy with phenytoin, carbamazepine, and stiripentol on formation of 4-ene-valproate, a hepatotoxic metabolite of valproic acid. Clin. Pharmacol. Ther. 48 (3), 225–235.

Loscher, W., 1978. Serum-protein binding and pharmacokinetics of Valproate in man, dog, rat and mouse. J. Pharmacol. Exp. Ther. 204 (2), 255–261.

Lundberg, B., Nergardh, A., Boreus, L.O., 1982. Plasma concentrations of Valproate during maintenance therapy in epileptic children. J. Neurol. 228 (2), 133–141.

Maharaj, A.R., Barrett, J.S., Edginton, A.N., 2013. A workflow example of PBPK modeling to support pediatric research and development: case study with lorazepam. AAPS J. 15 (2), 455–464.

McLaughlin, D.B., Andrews, J.A., Hooper, W.D., Cannell, G.R., Eadie, M.J., Dickinson, R.G., 2000. Apparent autoinduction of valproate beta-oxidation in humans. Br. J. Clin. Pharmacol. 49 (5), 409–415.

Morse, R.P., 2011. Dravet syndrome: inroads into understanding epileptic encephalopathies. J. Pediatr. 158 (3), 354–359.

Nitsche, V., Mascher, H., 1982. The pharmacokinetics of valproic acid after oral and parenteral administration in healthy-volunteers. Epilepsia 23 (2), 153–162.

Perucca, E., Gatti, G., Frigo, G.M., Crema, A., 1978a. Pharmacokinetics of Valproic acid after oral and intravenous administration. Br. J. Clin. Pharmacol. 5 (4), 313–318.

Perucca, E., Gatti, G., Frigo, G.M., Crema, A., Calzetti, S., Visintini, D., 1978b. Disposition of sodium Valproate in epileptic patients. Br. J. Clin. Pharmacol. 5 (6), 495–499.

Rodgers, T., Leahy, D., Rowland, M., 2005. Physiologically based pharmacokinetic modeling 1: Predicting the tissue distribution of moderate-to-strong bases. J. Pharm. Sci. 94 (6), 1259–1276.

Rodgers, T., Rowland, M., 2006. Physiologically based pharmacokinetic modelling 2: Predicting the tissue distribution of acids, very weak bases, neutrals and zwitterions. J. Pharm. Sci. 95 (6), 1238–1257.

Rowland, Yeo K., Jamei, M., Yang, J., Tucker, G.T., Rostami-Hodjegan, A., 2010. Physiologically based mechanistic modelling to predict complex drug–drug interactions involving simultaneous competitive and time-dependent enzyme inhibition by parent compound and its metabolite in both liver and gut – the effect of diltiazem on the time-course of exposure to triazolam. Eur. J. Pharm. Sci.: Off. J. Eur. Fed. Pharma. Sci. 39 (5), 298–309.

Sadeque, A.J.M., Fisher, M.B., Korzekwa, K.R., Gonzalez, F.J., Rettie, A.E., 1997. Human CYP2C9 and CYP2A6 mediate formation of the hepatotoxin 4-ene-valproic acid. J. Pharmacol. Exp. Ther. 283 (2), 698–703.

Salem, F., Johnson, T.N., Barter, Z.E., Leeder, J.S., Rostami-Hodjegan, A., 2013. Age related changes in fractional elimination pathways for drugs: assessing the impact of variable ontogeny on metabolic drug–drug interactions. J. Clin. Pharmacol. 53 (8), 857–865.

Scheyer, R.D., Cramer, J.A., Toftness, B.R., Hochholzer, J.M., Mattson, R.H., 1990. Invivo determination of Valproate binding constants during sole and multidrug therapy. Ther. Drug Monit. 12 (2), 117–123.

Soars, M.G., Burchell, B., Riley, R.J., 2002. In vitro analysis of human drug glucuronidation and prediction of in vivo metabolic clearance. J. Pharmacol. Exp. Ther. 301 (1), 382–390.

Suzuki, Y., Itoh, H., Abe, T., Nishimura, F., Sato, Y., Takeyama, M., 2011. No effect of co-administered antiepileptic drugs on in-vivo protein binding parameters of valproic acid in patients with epilepsy. J. Pharm. Pharmacol. 63 (7), 976–981.

Ueshima, S., Aiba, T., Ishikawa, N., Sato, T., Kawasaki, H., Kurosaki, Y., Ohtsuka, Y., Sendo, T., 2009. Poor applicability of estimation method for adults to calculate unbound serum concentrations of valproic acid in epileptic neonates and infants. J. Clin. Pharm. Ther. 34 (4), 415–422.

Ueshima, S., Aiba, T., Sato, T., Matsunaga, H., Kurosaki, Y., Ohtsuka, Y., Sendo, T., 2011. Empirical approach for improved estimation of unbound serum concentrations of Valproic acid in epileptic infants by considering their physical development. Biol. Pharm. Bull. 34 (1), 108–113.

Valentin, J., 2002. Basic anatomical and physiological data for use in radiological protection: reference values: ICRP publication 89. Ann. ICRP 32 (3–4), 1–277.

Visudtibhan, A., Bhudhisawadi, K., Vaewpanich, J., Chulavatnatol, S., Kaojareon, S., 2011. Pharmacokinetics and clinical application of intravenous valproate in Thai epileptic children. Brain Dev. 33 (3), 189–194.

West, G.B., Brown, J.H., Enquist, B.J., 1999. The fourth dimension of life: fractal geometry and allometric scaling of organisms. Science 284 (5420), 1677–1679.

West, G.B., Brown, J.H., Enquist, B.J., 1997. A general model for the origin of allometric scaling laws in biology. Science 276 (5309), 122–126.

Williams, J.H., Jayaraman, B., Swoboda, K.J., Barrett, J.S., 2012. Population pharmacokinetics of Valproic acid in pediatric patients with epilepsy: considerations for dosing spinal muscular atrophy patients. J. Clin. Pharmacol. 52 (11), 1676–1688.

Zaccara, G., Messori, A., Moroni, F., 1988. Clinical pharmacokinetics of valproic acid–1988. Clin. Pharmacokinet. 15 (6), 367–389.